The Ran pathway uniquely regulates cytokinesis depending on cell fate in *C. elegans* embryos

Imge Özügergin, Karina Mastronardi, Alisa Piekny

Department of Biology, Concordia University, Montreal, Quebec, Canada

Piekny Lab

ABSTRACT

Cytokinesis is required to complete division, and must be tightly regulated to prevent aneuploidy and cell fate changes. Microtubule-dependent and –independent mechanisms regulate cytokinesis, and reliance on a pathway varies based on cell size, shape or fate. We found that Ran-GTP regulates the localization of human anillin (*C. elegans* ANI-1), a core component of the cytokinetic ring. During mitosis, a Ran-GTP gradient is maintained with high levels around chromatin and low levels in the cytosol. This is because the RanGEF RCC1 (*C. elegans* RAN-3) is tethered to chromatin, while RanGAP (*C. elegans* RAN-2) is cytoplasmic. Our model is that importin-α/-β binds to the nuclear localization signals of cortical regulators to facilitate their localization and function for cytokinesis, and position the ring away from chromatin. To determine if requirements for the Ran pathway differs depending on cell fate, we studied cytokinesis in the early *C. elegans* embryo. The fertilized embryo divides asymmetrically to give rise to an anterior AB daughter fated to be multiple tissues, and a posterior P1 daughter fated to be germline. Imaging with high temporal resolution revealed that each cell has unique ingression kinetics, supported by differences in the accumulation of contractile proteins. Lowering Ran-GTP levels via RAN-3 RNAi increased ingression kinetics in both AB and P1 cells, which was suppressed by co-depletion of the contractility regulators ECT-2 (RhoA-GEF) or LET-502 (Rho Kinase). Interestingly, co-depletion of ANI-1 suppressed RAN-3 phenotypes in AB, but not P1 cells, suggesting that they have different pathway requirements. This is supported by different requirements for importin-α (IMA-3) and -β (IMB-1) in AB vs. P1 cells. We are currently using CRISPR to generate mutations in ANI-1 that disrupt importin-binding. Our findings reveal differences in mechanisms regulating cytokinesis in cells with different fates and emphasize the need to study cytokinesis *in vivo*.

INTRODUCTION

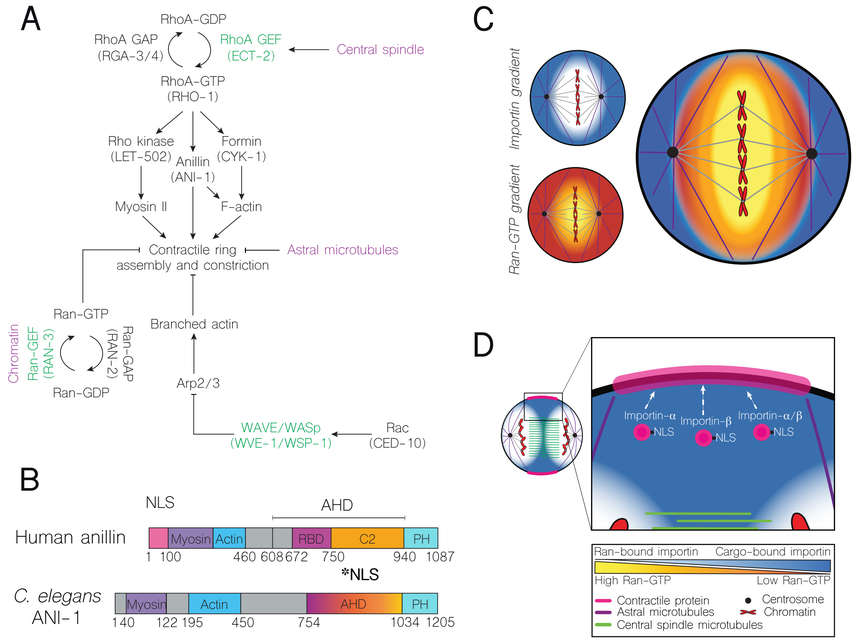

Figure 1. **A)** Pathways that regulate the contractile ring for cytokinesis include spindle-dependent mechanisms and chromatin-associated Ran-GTP. Ran may modulate cortical contractility in *C. elegans* embryos by dictating where importins are free to bind NLS-containing cargo. Ran could regulate the localization and activity of NLS-containing proteins such as ECT-2, WSP-1 and ANI-1. **B)** Cartoons show the binding domains in human anillin and ANI-1, the *C. elegans* homologue [myosin; purple, actin; blue, RhoA-GTP binding domain (RBD); magenta, C2; orange, pleckstrin homology domain (PH); blue, and nuclear localization signals (NLS)]. The RBD and C2 domain are also collectively known as the AHD (anillin homology domain). Other NLS-containing cytokinesis regulators that could be regulated by importins include ECT-2 and WSP-1. **C)** *Left:* The importin gradient (blue, top) and Ran gradient (orange, bottom) that run opposite to each other within a cell are shown separately. *Right:* The cell depicts both gradients combined in a metaphase cell. **D)** A cartoon schematic shows how a gradient of importins free from Ran-GTP forms near the equatorial cortex during anaphase, where it influences the localization of contractile ring components, together with RhoA and MTs (microtubules). In anaphase, the two separating Ran gradients lead to a zone of importin activity at the equatorial cortex. Here, importins help position the division plane by binding to contractile proteins (such as anillin) and facilitating their localization to the cortex. Legend shows both gradients and lists components of the cell. *ANI-1 has been shown to bind human importin-β.

RESULTS

Ingression varies depending on cell fate

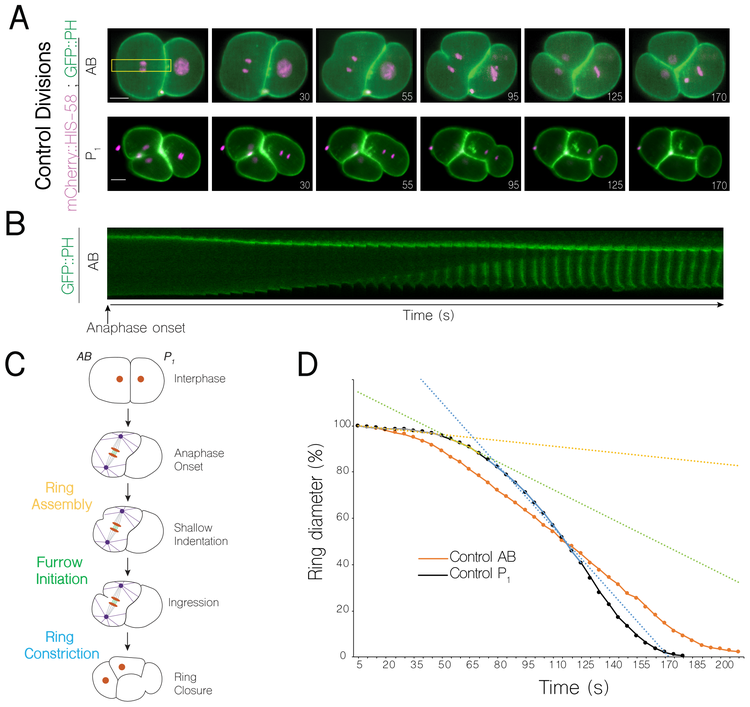

Figure 2. **A)** Timelapse images of control *C. elegans* embryos expressing mCherry::HIS-58 (magenta) and GFP::PH (green) during the AB (top) and P_1 (bottom) division are shown. Times are shown after anaphase onset in seconds. **B)** Kymographs taken from a box drawn at the division plane (example in A) are shown for the AB (top) and P_1 (bottom) division, at 5-second intervals from anaphase onset until closure. **C)** A cartoon schematic shows the different phases of ingression. These were determined as shown in D. **D)** A graph shows the average rates of AB-cell and P_1-cell ring closure. Tangents are drawn to show the transition for each phase (yellow: ring assembly, green: furrow initiation, blue: ring constriction) until 40% ring diameter.

Switching cell fate changes ingression kinetics

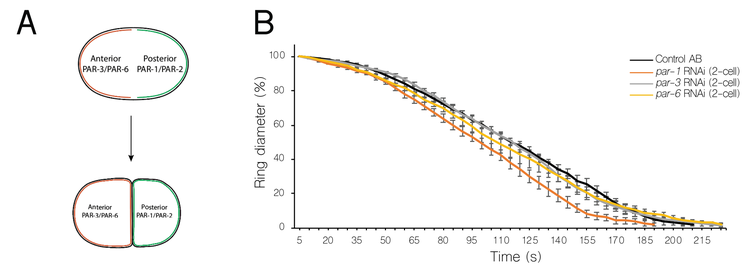

Figure 3. **A)** A cartoon shows mutually exclusive distribution of PAR proteins, which sets up polarity in the one-cell embryo. **B)** A graph shows the average rates of ring closure for control AB-cells (black) and *par-1* (orange), *par-3* (grey), and *par-6* (yellow) depleted 2-cell embryos, with ring diameter (as %) on the Y-axis, and time in seconds on the X-axis. Error bars for all graphs show SEM.

The Ran pathway influences cortical activity during anaphase

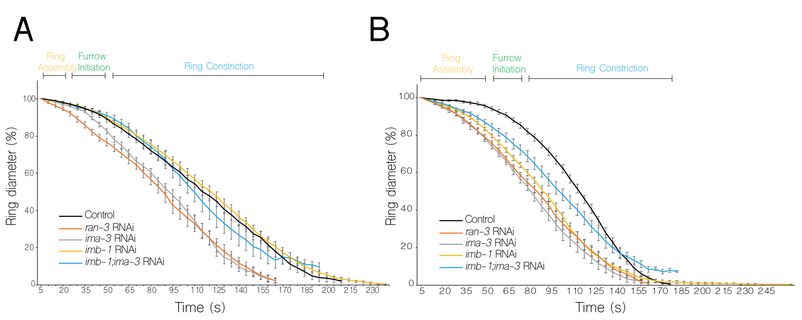

Figure 4. **A)** A graph shows the average rates of AB-cell ring closure for control (black), *ran-3* RNAi (orange), *ima-3* RNAi (grey), *imb-1* RNAi (yellow) and *imb-1; ima-3* RNAi (blue) cells, with ring diameter (as %) on the Y-axis, and time in seconds on the X-axis. **B)** A graph shows the average rates of P_1-cell ring closure for control (black), *ran-3* (orange), *ima-3* (grey), *imb-1* (yellow) and *imb-1; ima-3* (blue) depleted embryos, with ring diameter (as %) on the Y-axis, and time in seconds on the X-axis. Error bars for all graphs show SEM.

Ran-GTP depletion decreases duration of the ring assembly phase

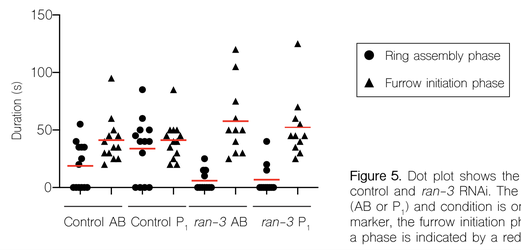

Figure 5. Dot plot shows the duration of the ring assembly and furrow initiation phases for control and *ran-3* RNAi. The duration of each phase is in seconds on the Y-axis, cell type (AB or P_1) and condition is on the X-axis. The ring assembly phase is shown using a circle marker, the furrow initiation phase is shown using a triangle marker. The average duration of a phase is indicated by a red line.

Ran-GTP depletion changes breadth of actin localization

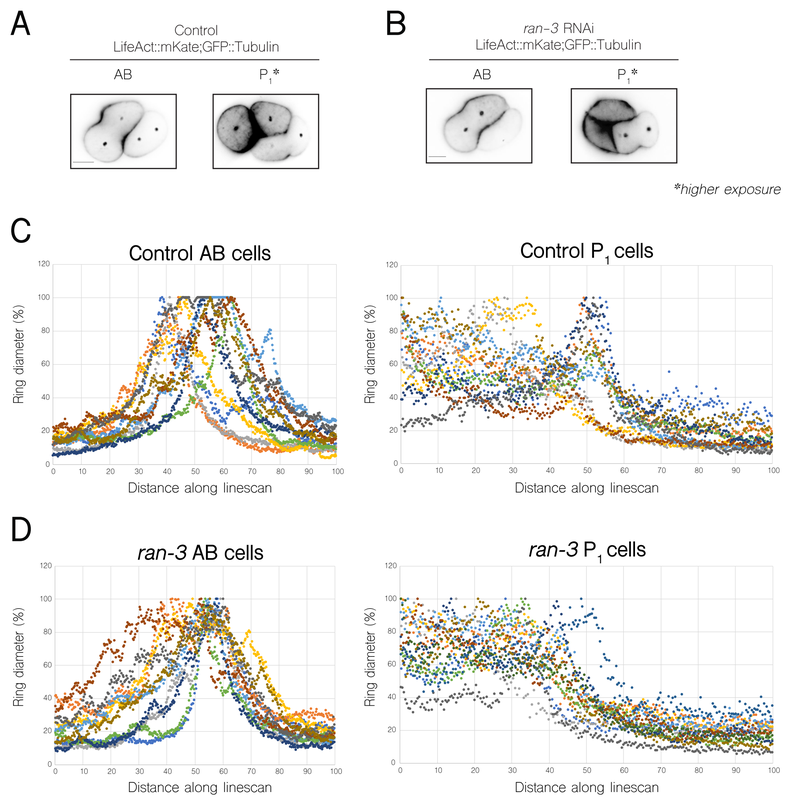

Figure 6. **A)** Images show actin localization in control AB (left) and P1 (right) cells expressing LifeAct::mKate2 (magenta) and GFP::tubulin (green). **B)** Images show actin localization in *ran-3* AB (left) and P1 (right) cells expressing LifeAct::mKate2 (magenta) and GFP::tubulin (green). **C)** Graphs show the rates of AB-cell (left) and P_1-cell (right) ring closure for control cells. **D)** Graphs shows the rates of AB-cell (left) and P_1-cell (right) ring closure under *ran-3* RNAi treatment. Ring diameter is shown (as %) on the Y-axis, and distance along the linescan (as %) on the X-axis. One-pixel wide linescans were drawn from pole to pole.

Ran regulation of cytokinesis differs between cells

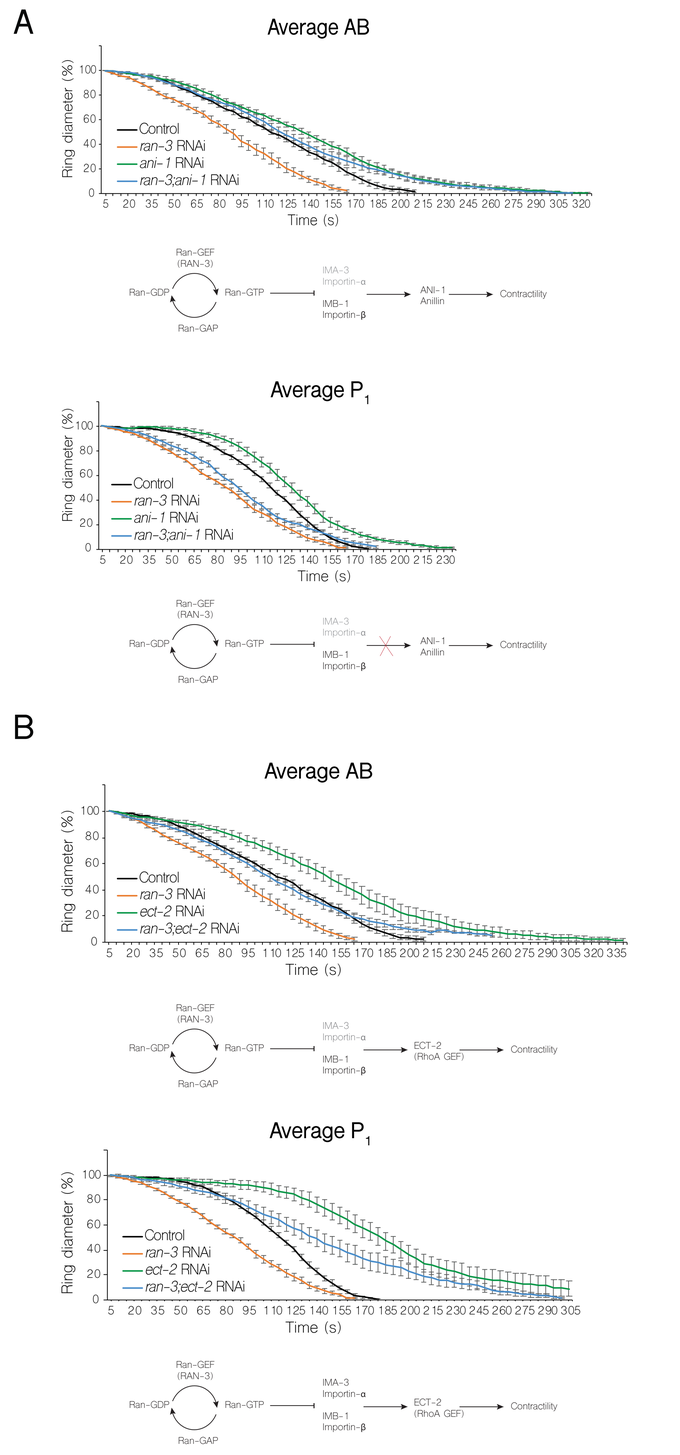

Figure 7. **A)** Graphs show the average ingression kinetics in AB (top) and P_1 (bottom) cells in control (black), *ran-3* (orange), *ani-1* (green), and *ran-3; ani-1* (blue) RNAi conditions, with ring diameter (as %) on the Y-axis, and time in seconds on the X-axis. **B)** Graphs show the average ingression kinetics in AB (left) and P_1 (right) cells in control (black), *ran-3* (orange), *ect-2* (green), and *ran-3; ect-2* (blue) RNAi conditions, with ring diameter (as %) on the Y-axis, and time in seconds on the X-axis. The hypothesized pathway of Ran regulation are shown below each graph. Error bars for all graphs show SEM.

Model of Ran regulation

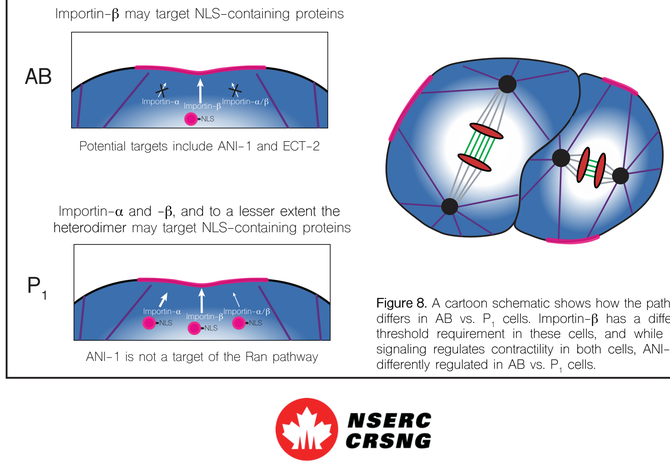

Figure 8. A cartoon schematic shows how the pathway differs in AB vs. P_1 cells. Importin-β has a different threshold requirement in these cells, and while Ran signaling regulates contractility in both cells, ANI-1 is differently regulated in AB vs. P_1 cells.

NSERC CRSNG